

Pressure Shifts and Pressure Broadening of the B and γ Bands of Oxygen

John E. Barnes* and Paul B. Hays†

*NOAA/Climate Monitoring and Diagnostics Laboratory/Mauna Loa Observatory, Hilo, Hawaii 96721; and †Department of Atmospheric, Oceanic and Space Physics, University of Michigan, Ann Arbor, Michigan 48109

Received April 16, 2002; in revised form August 20, 2002

Measurements of pressure shift and pressure broadening in molecular oxygen have been made for rotational transitions in the B ($1 \leftarrow 0$) and γ ($2 \leftarrow 0$) vibrational bands of the $b^1\Sigma_g^+ \leftarrow X^3\Sigma_g^-$ visible electronic transition. The absorption features were measured simultaneously in two cells by photoacoustic spectroscopy using a scanning dye laser. The measurements were made with background gases of both pure oxygen and air at room temperature. The pressure shifts were all negative. The measurements show the magnitude of the pressure shift increasing with vibrational quantum number when compared with existing data for the A ($0 \leftarrow 0$) band. The shifts also increase with rotational number within each vibrational band. The shifts in air are larger than in oxygen although the difference gets smaller with vibrational number. The average shifts in air for the A, B, and γ bands were 36, 11, and 0.2% higher, respectively, than in pure oxygen. The pressure broadening of the rotational lines does not change significantly with vibrational number and in general decreases with rotational number within a band. The pressure shift measurements were used by the high-resolution Doppler imager (on the Upper Atmospheric Research Satellite) to correct the Doppler wind measurements. © 2002 Elsevier Science (USA)

INTRODUCTION

The $b^1\Sigma_g^+ \leftarrow X^3\Sigma_g^-$ visible electronic transition in molecular oxygen is quite weak and was first identified by absorption in the atmosphere. The radiation is due to a magnetic dipole transition (I) a from singlet upper state to the triplet ground state. The linestrength decreases quickly with vibrational quantum number. The strengths for the A, B, and γ bands are 532, 40.8, and $1.52 \text{ cm}^{-1}/\text{km}/\text{atm}$, respectively (2–4). There have been many applications using these absorption lines for atmospheric research. Absorption of solar radiation has a significant effect on the tropopause region (5) and middle atmosphere (6). Doppler shifts of these lines in both absorption and emission have been used by the high-resolution Doppler imager (on the Upper Atmospheric Research Satellite) for wind measurements (7). Pressure shift and pressure broadening of the lines must be taken into account in the analysis of the spectral data received by the instrument and were the main reason for undertaking this study. For this reason it was important to measure the broadening in air (O_2 -air) as well as self-broadening in oxygen (O_2 - O_2). Possible future applications include aerosol distribution measurements (8), cloud structure (9), and cloud top height and coverage (10).

Extensive A-band ($0-0$, 762 nm, $13\,120 \text{ cm}^{-1}$) measurements of both pressure shift and broadening were made by Ritter (11). The measurements were made under various temperatures and background gases including O_2 , air, and the noble gases. Some of these data were not published in a refereed journal and have been listed in this work for the convenience of the reader and for comparison to this work's B ($1-0$, 688 nm, $14\,535 \text{ cm}^{-1}$)-

and γ ($2-0$, 629 nm, $15\,898 \text{ cm}^{-1}$)-band data. No A-band measurements were performed in this work.

EXPERIMENT

In this work pressure shift and broadening of O_2 in the B and γ bands have been measured in air (O_2 -air) and in pure oxygen (O_2 - O_2). All measurements were made at room temperature (23 C). No effort was made to measure line positions or relative intensities. The strength of the signal for a given line and its separation from neighboring lines determined which could be measured with significant enough accuracy to be included in this work. Measurements of oxygen lines in air had signal strength five times lower (and higher errors) than those made in pure oxygen.

The measurements of relatively weak absorption features were performed by photoacoustic spectroscopy (PAS) (13). A schematic of the experimental apparatus is shown in Fig. 1. The laser used was a Coherent CR-699-21 ring dye laser with a typical linewidth of 0.0007 cm^{-1} (20 MHz). Typical power levels were 100 mW (B band) and 400 mW (γ band). The laser had a built-in wavemeter and scanning was controlled by a computer. Power was monitored by the wavemeter to correct for fluctuations of the laser during the scan of a single line. The laser beam was modulated by a mechanical chopper at about 95 Hz, which optimized the signal-to-noise ratio in the photoacoustic cells. The PAS cells were made out of blocks of aluminum 12.7 cm long and about 5 cm square. They were optimized for nonresonant conditions by keeping the volume to a minimum. A 1.27-cm-diameter hole was bored through the block to form the

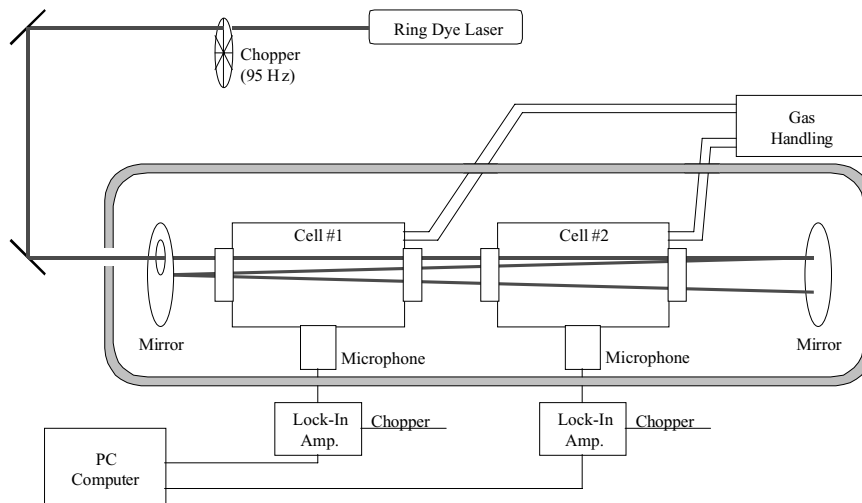


FIG. 1. Experimental apparatus. The two photoacoustic cells were in a 20-pass cavity.

cavity. The microphone was mounted on top of the block and was connected to the cavity by a pinhole. The microphones were made by Bruel and Kjaer (2.54 cm diameter) and had a sensitivity of 0.1 V/dyn/cm². The ends of the cavity were covered by 2.54-cm-diameter windows with anti-reflection coatings.

In order to increase the light intensity in each of the PAS cells, both cells were mounted between two concave mirrors aligned to pass the beam through each cell 20 times. A small off-axis hole in one of the mirrors allowed entrance of the beam. Positioning both cells in the same cavity eliminated any error due to measuring the power in each cell independently. Measuring both cells simultaneously also eliminated the errors in laser wavelength, that would be present if only one cell were used for the reference and then refilled and rescanned for the sample condition. Because the absorption by oxygen in these bands is so small, the loss of light is dominated by window and mirror losses. The absorption in one cell does not significantly affect the power in the other. This was tested by looking for changes in the lineshape of one cell, when pressure was changed in the other. None were found within experimental error. The mirror cavity and the cells were enclosed in a box lined with acoustic absorbing foam to minimize external acoustical noise. The laser, chopper, cells, and box were all mounted on a single optical table with pneumatic vibration isolation.

Two lock-in amplifiers were used for the signals from the microphones, an Ithaco 399 stand-alone and a PC plug-in Ithaco 3981. The signal from the chopper was used as the lock-on frequency. Because of the different time constants of the amplifiers an offset in peak position was introduced, which had to be accounted for in the analysis. The offset was precisely measured by feeding the signal from one cell into both lock-in amplifiers. Repeated scans at different time constants were also made to ensure that the peak width was accurate. A personal computer that was triggered by the laser control computer at the beginning of a scan was used for data acquisition. Photoacoustic absorption

cells can be designed to be used in resonant modes or in a non-resonant mode. In the resonant mode cell the beam is chopped at an acoustically resonant frequency and the acoustic signal is amplified. The tradeoff is that the response of the cell decreases with frequency. Modeling and measurements of the two designs determined that the nonresonant cell would give the best performance. The modeling followed Ritter (11) and agreed with measured cell response to within a factor of 2.

Each line was measured between 5 and 10 times and curve fits were performed on each of the measurements. The standard deviation of these measurements was used for the error. The pressure dependence was found by pressurizing one cell with 320 to 347 hPa of O₂ and holding the other to 993 hPa (ambient) of O₂ as a reference. A linear extrapolation was then made to one atmosphere. The linear dependence of both shift and width on pressure was demonstrated by (11).

The reference and sample lineshapes that were simultaneously measured for each vibrational-rotational line were each fitted with a restricted Voigt profile. A Voigt profile is the convolution of a gaussian temperature (Doppler)-broadened profile and a collision (Lorentz)-broadened profile:

$$H(a, u) = a/\pi \int_{-\infty}^{\infty} \exp(-y^2)/(a^2 + (u - y)^2) dy, \quad [1]$$

where

$$a = \Gamma/(4\pi \Delta v_D), \quad [2]$$

$$u = (v - v_0)/\Delta v_D \quad [3]$$

$$\Delta v_D = v_0/c(2kT/m_a)^{0.5}. \quad [4]$$

In these expressions, k is the Boltzmann constant, c is the speed of light, T is the temperature, v_0 is the center

TABLE 1
Pressure Shift in Oxygen ($\text{cm}^{-1}/\text{atm}$): Numbers in Parentheses Represent Two Standard Deviations in Units of the Least Significant Digit (A-Band Data from Ritter (11))

$\Delta N \Delta J$	N''	J''	A Band (O ₂)	A Band (Air)	B Band (O ₂)	B Band (Air)	γ Band (O ₂)	γ Band (Air)
PP	25	25	-0.0064					
PQ	25	24						
PP	23	23						
PQ	23	22						
PP	21	21		-0.0083				
PQ	21	20		-0.0083				
PP	19	19	-0.0059	-0.0081	-0.0083(10)	-0.0087(13)		
PQ	19	18	-0.0056	-0.0080	-0.0091(8)	-0.0099(12)		
PP	17	17	-0.0057	-0.0078	-0.0093(5)	-0.0102(6)	-0.0121(19)	
PQ	17	16	-0.0058	-0.0077	-0.0085(3)	-0.0093(6)	-0.0099(16)	
PP	15	15	-0.0058	-0.0074	-0.0084(8)	-0.0094(9)	-0.0104(16)	
PQ	15	14	-0.0056	-0.0077	-0.0084(7)	-0.0091(9)	-0.0121(19)	
PP	13	13	-0.0053	-0.0078	-0.0083(5)	-0.0090(6)	-0.0101(9)	-0.0100(19)
PQ	13	12	-0.0055	-0.0074	-0.0081(2)	-0.0088(6)	-0.0113(19)	-0.0114(13)
PP	11	11	-0.0053	-0.0074	-0.0080(8)	-0.0088(8)	-0.0099(8)	-0.0097(20)
PQ	11	10	-0.0053	-0.0073	-0.0085(6)	-0.0092(6)	-0.0109(17)	-0.0097(5)
PP	9	9	-0.0055	-0.0073	-0.0083(6)	-0.0092(6)	-0.0107(12)	-0.0112(12)
PQ	9	8	-0.0052	-0.0073	-0.0082(11)	-0.0089(12)	-0.0102(13)	-0.0093(24)
PP	7	7	-0.0053	-0.0072	-0.0085(2)	-0.0092(2)	-0.0094(15)	-0.0095(9)
PQ	7	6	-0.0052	-0.0069	-0.0074(3)	-0.0081(4)	-0.0097(21)	-0.0095(13)
PP	5	5	-0.0048	-0.0068	-0.0078(3)	-0.0086(6)	-0.0093(16)	-0.0092(9)
PQ	5	4	-0.0048	-0.0066	-0.0076(5)	-0.0085(7)	-0.0083(24)	-0.0087(34)
PP	3	3	-0.0045	-0.0059	-0.0059(3)	-0.0069(7)	-0.0084(21)	-0.0091(27)
PQ	3	2	-0.0043	-0.0056	-0.0058(7)		-0.0066(41)	
PP	1	1	-0.0028	-0.0038	-0.0039(3)		-0.0055(28)	
RR	1	1	-0.0016		-0.0038(12)		-0.0025(77)	
RQ	1	2	-0.0025		-0.0054(4)		-0.0074(28)	
RR	3	3	-0.0026		-0.0066	-0.0077(9)		
RQ	3	4	-0.0032		-0.0062(2)	-0.0073(12)	-0.0074(9)	-0.0079(22)
RR	5	5	-0.0038		-0.0062(3)	-0.0074(7)	-0.0087(10)	-0.0086(25)
RQ	5	6	-0.0039		-0.0067(1)	-0.0077(3)		
RR	7	7	-0.0043		-0.0067(2)		-0.0095(7)	-0.0102(22)
RQ	7	8	-0.0043				-0.0085(5)	-0.0087(22)
RR	9	9	-0.0046				-0.0099(7)	-0.0090(16)
RQ	9	10	-0.0044					
RR	11	11	-0.0048					
RQ	11	12	-0.0047					
RR	13	13	-0.0052					
RQ	13	14	-0.0053					
RR	15	15	-0.0059					
RQ	15	16	-0.0055					
RR	17	17	-0.0058					
RQ	17	18						
RR	19	19						
RQ	19	20	-0.0060					
RR	21	21	-0.0064					
RQ	21	22						
RR	23	23	-0.0066					
RQ	23	24	-0.0065					
RR	25	25						
RQ	25	26	-0.0065					

wavelength, m_a is the molecular mass, and Γ is the Lorentz width. The Doppler width, $\Delta\nu_D$, is multiplied by $(\ln 2)^{0.5}$ to get the HWHM (half width half maximum). The fit was restricted by fixing the Doppler width parameter. This allowed comparison of the results to other studies, which also fixed the Doppler width (3, 14). The Doppler HWHM was fixed at 0.0158 cm^{-1} for the B band and 0.0173 cm^{-1} for the γ band, corresponding to oxygen at room temperature. The curve fit software used was the IDL Version 5.4 written by Research Systems Inc. Documentation can be found in Rybicki and Lightman (15). Besides the three Voigt parameters that were fit (height, peak center, Lorentz width), a constant background was also fit. The constant background accounted for experimental noise in the measurement but was not used for any results. The reference and sample profiles for each scan were both fit for the Voigt lineshape. The pressure shift per atmosphere was proportional to the difference between the center wavelengths of the two fits.

The data were also analyzed using a simple Lorentz profile for the curve fit. The pressure shift results were nearly the same as with the Voigt fit, but the linewidths were all larger. This would be expected since the Doppler width accounts for a portion of the linewidth in a Voigt profile. The Lorentz results are available from the authors upon request.

RESULTS AND DISCUSSION

The pressure shifts in air and in oxygen have been listed in Table 1 for the A, B, and γ bands. The A-band data are taken from Ritter (11). The shifts in oxygen (self-broadening) are shown in Fig. 2. The magnitude of the shift increases with vibrational quantum number. The same general behavior of increasing magnitude of the shift with rotational number, is seen for all three bands. In Fig. 3 the ratio of the shift in air to the shift in oxygen is plotted. The average ratio for the A band seen by Ritter (11) is significantly larger than the average shift in the

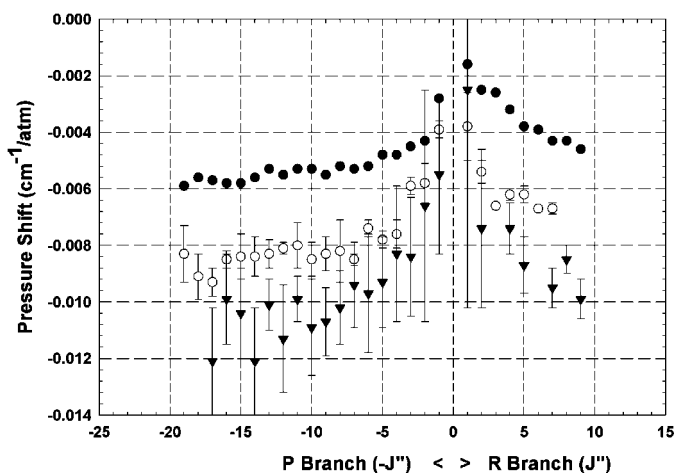


FIG. 2. Pressure shift in oxygen (self-broadening): filled circles, A band; open circles, B band; filled triangles, γ band.

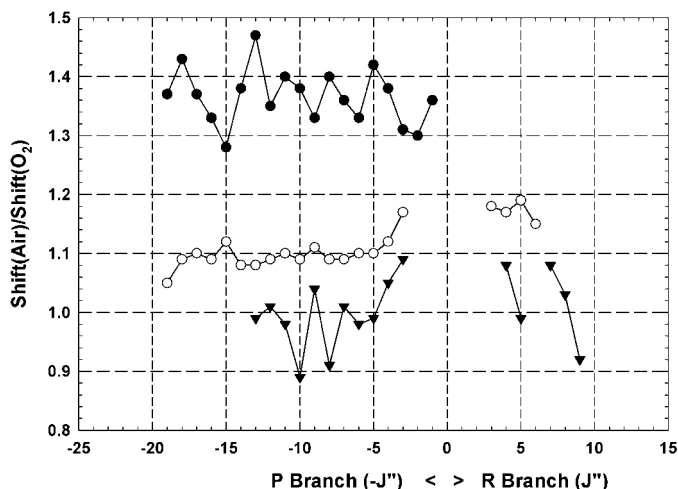


FIG. 3. Ratio of pressure shift in air to shift in oxygen: filled circles, A band; open circles, B band; filled triangles, γ band.

B and γ bands found in this work and the γ -band ratios are not significantly different from zero. The average ratios for all the A, B, and γ band lines are 1.36(0.094), 1.113(0.074) and 1.002(0.120), respectively, with two standard deviations shown in parentheses.

In Table 2 results with previous works are tabled with this work's for comparison. Four experimental methods are used: photoacoustic spectroscopy (this work, 11, 12); intercavity laser absorption (14); white cell (3); Fourier transform spectroscopy (17, 18, 20). The same lines are averaged within a band except for (20) which presented only fitted spectral parameters for the entire band and (21). The A-band studies using air (11, 12) as a colliding gas are tabled with two studies (17, 18) using N_2 . The four measurements in oxygen are paired with a factor of 2 difference between the two pairs and do not agree within experimental error, as noted by Brown and Plymate (17). This large a difference would not be attributable to the small difference expected between air and N_2 used as the colliding gas. The B-band self-shift of this work is the lower of the other two measurements (18, 20). A factor of 2 difference is also apparent between this work and (18) and is significant within experimental error. The γ -band shift is much lower than the only comparable measurement (20).

The pressure broadening (Lorentz width parameter) of the Voigt fits in oxygen is listed in Table 3 and plotted in Fig. 4. The broadening is very similar for the A, B, and γ bands and agrees within experimental error. The broadening in all three bands decreases with rotational quantum number. The decrease in broadening with rotational quantum number agrees qualitatively with calculations in the microwave (16). In Fig. 5 the ratio of the width in air to the width in O_2 is plotted. The effect of air on the width appears to increase with rotational quantum number but there is large scatter in the data. The averages for all lines in the A, B, and γ bands are 1.018(0.027), 1.029(0.071), and 1.074(0.075), respectively, with two standard deviation shown in parentheses.

TABLE 2
Comparison of Broadening and Shift with Previous Work^d

Self broadening (cm ⁻¹ /atm)	Broad (N ₂ , air)/ Broad (O ₂)	Self shift (cm ⁻¹ /atm)	Shift (N ₂ , air)/ Shift (O ₂)	Reference
A Band		P5Q4 through P17P17 averaged		
0.0484(5)	1.016(32) ^a	-0.0054(6)	1.37(10)	(11, 12)
0.0475(12)	1.011	-0.0053(8)	1.11	(17)
		-0.0107(20)	1.71	(18)
0.069(5)		-0.0110(25)		(20) ^b
B Band		P5Q4 through P17P17 averaged		
0.0470(12)	1.018(54)	-0.0082(5)	1.10(3)	This work (3)
0.0523(14)		-0.0157(40)		(18)
		-0.0110(45)		(20) ^b
0.0740(200)				
γ Band		P5Q4 through P13P13 averaged		
0.0497(32)	1.079(49)	-0.0100(15)	0.98(10)	This work (14)
0.0513				(20) ^b
0.0830(120)		-0.0380(120)		(21)
		-0.0077 ^c		

^a P1P1, P3Q2, P7P7, P15P15, P21P21 averaged for air.

^b Shift determined by spectral parameter fits of all lines measured, Lorentz curve shape used for fit.

^c Indirect measurement, asymmetry modeling for oxygen in air.

^d Numbers in parentheses represent two standard deviations of the averaged lines, in units of the least significant digit or are taken from the reference.

A comparison of average broadening with other measurements is shown in Table 2. The values agree across the three bands except for (20), which has substantially larger widths. The difference in part is due to the Lorentz lineshape used as a fitting function in (20), which would result in a greater width than the Voigt fit parameter.

The average pressure shifts measured for the A, B, and γ bands are -0.0071, -0.0087, and -0.0095 cm⁻¹/atm, respectively. These shifts have to be accounted for in the analysis of the high resolution Doppler imager's winds since they will add

or subtract to the Doppler shifts seen by the imager as winds. The pressure shifts at one atmosphere are equivalent to Doppler shifts of 162, 179, and 179 m/s, but the imager measured at much lower pressures. At the tropopause (about 15 km) the pressure is 0.1 atm and the pressure shift would be about 17 m/s, which is on the same order as terrestrial winds at that altitude. At 0.01 atm (about 30 km) the correction is 1.7 m/s, which may still be significant. At the stratopause, 0.001 atm (about 50 km), and above the correction would be 0.17 m/s and would be insignificant.

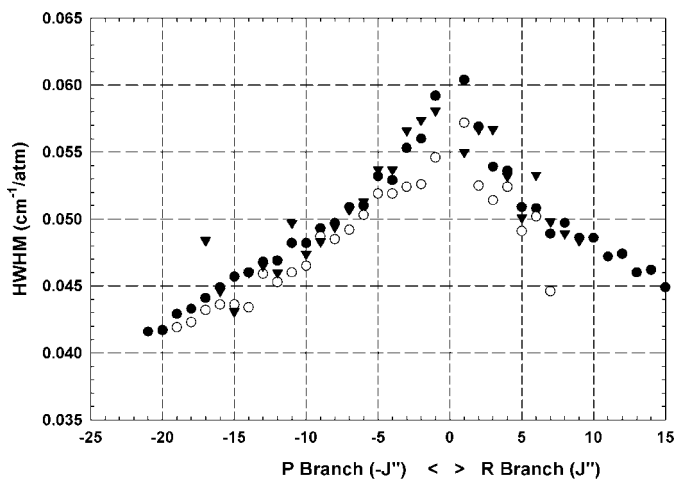


FIG. 4. Lorentz broadening in one atmosphere of oxygen (self-broadening): filled circles, A band; open circles, B band; filled triangles, γ band.

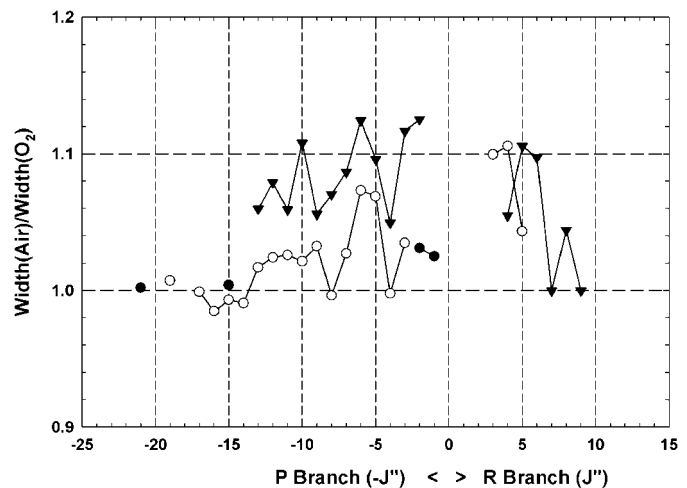


FIG. 5. Ratio of broadening in air to self-broadening in oxygen: filled circles, A band; open circles, B band; filled triangles, γ band.

TABLE 3
 Pressure Broadening (Lorentz Parameter) in Oxygen (HWHM, $\text{cm}^{-1}/\text{atm}$): Numbers in Parentheses Represent Two Standard Deviations in Units of the Least Significant Digit (A-Band Data from Ritter (11))

$\Delta N \Delta J$	N''	J''	A Band (O ₂)	A Band (Air)	B Band (O ₂)	B Band (Air)	γ Band (O ₂)	γ Band (Air)
PP	29	29	0.0362					
PQ	29	28	0.0354					
PP	27	27	0.0371					
PQ	27	26	0.0372					
PP	25	25	0.0390					
PQ	25	24	0.0387					
PP	23	23	0.0400					
PQ	23	22	0.0404					
PP	21	21	0.0416	0.0415				
PQ	21	20	0.0417					
PP	19	19	0.0429		0.0419(17)	0.0422(17)		
PQ	19	18	0.0433		0.0423(10)			
PP	17	17	0.0441		0.0432(5)	0.0432(5)	0.0484(42)	
PQ	17	16	0.0449		0.0436(19)	0.0430(25)	0.0446(69)	
PP	15	15	0.0457	0.0460	0.0436(10)	0.0433(12)	0.0431(35)	
PQ	15	14	0.0460		0.0434(9)	0.0430(10)	0.0460(35)	
PP	13	13	0.0468		0.0459(6)	0.0467(8)	0.0465(20)	0.0492(28)
PQ	13	12	0.0469		0.0453(4)	0.0464(6)	0.0460(32)	0.0497(48)
PP	11	11	0.0482		0.0460(5)	0.0471(6)	0.0497(24)	0.0526(25)
PQ	11	10	0.0482		0.0465(5)	0.0475(5)	0.0474(30)	0.0525(35)
PP	9	9	0.0493		0.0487(8)	0.0503(10)	0.0483(29)	0.0510(38)
PQ	9	8	0.0497		0.0485(13)	0.0484(14)	0.0494(19)	0.0529(26)
PP	7	7	0.0509	0.0524	0.0492(35)	0.0505(35)	0.0507(33)	0.0551(37)
PQ	7	6	0.0510		0.0503(4)	0.0540(5)	0.0513(37)	0.0577(45)
PP	5	5	0.0532		0.0519(7)	0.0554(11)	0.0537(33)	0.0588(48)
PQ	5	4	0.0529		0.0519(34)	0.0518(54)	0.0537(62)	0.0563(70)
PP	3	3	0.0553		0.0524(13)	0.0542(7)	0.0566(79)	0.0632(104)
PQ	3	2	0.0560	0.0574	0.0526(8)		0.0574(88)	0.0646(107)
PP	1	1	0.0592	0.0606	0.0546(9)		0.0581(110)	
RR	1	1	0.0604		0.0572(14)		0.0550(157)	
RQ	1	2	0.0569		0.0525(6)		0.0567(86)	
RR	3	3	0.0539		0.0514	0.0565(13)	0.0567(80)	
RQ	3	4	0.0536		0.0524(7)	0.0579(10)	0.0532(31)	0.0561(48)
RR	5	5	0.0509		0.0491(10)	0.0513(11)	0.0501(35)	0.0554(52)
RQ	5	6	0.0508		0.0502(8)		0.0533(26)	0.0584(34)
RR	7	7	0.0489		0.0446(2)		0.0498(27)	0.0498(39)
RQ	7	8	0.0497				0.0489(15)	0.0511(22)
RR	9	9	0.0486				0.0484(28)	0.0484(34)
RQ	9	10	0.0486					
RR	11	11	0.0472					
RQ	11	12	0.0474					
RR	13	13	0.0460					
RQ	13	14	0.0462					
RR	15	15	0.0449					
RQ	15	16	0.0449					
RR	17	17	0.0433					
RQ	17	18	0.0431					
RR	19	19	0.0422					
RQ	19	20	0.0419					
RR	21	21	0.0406					
RQ	21	22						
RR	23	23	0.0399					
RQ	23	24	0.0395					
RR	25	25						
RQ	25	26	0.0376					
RR	27	27	0.0366					

ACKNOWLEDGMENTS

The authors thank Frank Lee for his dye laser expertise and Sebastian Bronner for curve fitting analysis and acknowledge the financial support of the work by NASA, Upper Atmospheric Research Satellite.

REFERENCES

1. J. H. van Vleck, *Astrophys. J.* **80**, 161–170 (1934).
2. J. H. Miller, R. W. Boese, and L. P. Giver, *J. Quant. Spectrosc. Radiat. Transfer* **9**, 1507–1517 (1969).
3. L. P. Giver, R. W. Boese, and J. H. Miller, *J. Quant. Spectrosc. Radiat. Transfer* **14**, 793–802 (1974).
4. J. H. Miller, L. P. Giver, and R. W. Boese, *J. Quant. Spectrosc. Radiat. Transfer* **16**, 595 (1976).
5. J. Kiehl and T. Yamanouchi, *Tellus B* **37**, 1–6 (1985).
6. M. G. Mlynczak and B. T. Marshall, *J. Geophys. Res.* **23**, 657–660 (1996).
7. P. B. Hays, V. J. Abreu, M. E. Dobbs, D. A. Gell, H. J. Grassl, and W. R. Skinner, *J. Geophys. Res.* **98**, 713–723 (1993).
8. S. Petelina and D. Murtagh, Biennial Report, International Meteorological Institute in Stockholm, pp. 37. (1999–2000).
9. A. B. Davis, A. Marshak, E. Kassinov, and G. M. Stokes, *EOS Trans. Am. Geophys. Union*, 622–624 (1999).
10. A. Kuze and K. V. Chance, *J. Geophys. Res.* **99**, 14 481–14 491 (1994).
11. K. J. Ritter, “A High-Resolution Spectroscopic Study of Absorption Line Profiles in the A-Band of Molecular Oxygen.” Dissertation, University of Maryland, 1986.
12. K. J. Ritter and T. D. Wilkerson, *J. Mol. Spectrosc.* **121**, 1–19 (1987).
13. A. G. Bell, *Philos. Mag.* **11**, 510 (1881).
14. M. A. Melieres, M. Chenevier, and F. Stoeckel, *J. Quant. Spectrosc. Radiat. Transfer* **33**, 337–345 (1985).
15. G. B. Rybicki and A. P. Lightman, “Radiative Processes in Astrophysics.” Wiley–Interscience, New York, 1979.
16. E. W. Smith and M. Giraud, *J. Chem. Phys.* **71**, 4209–4217 (1979).
17. L. R. Brown and C. Plymate, *J. Mol. Spectrosc.* **199**, 166–179 (2000).
18. A. J. Phillips and P. A. Hamilton, *J. Mol. Spectrosc.* **174**, 587–594 (1995).
19. A. J. Phillips, F. Peters, and P. A. Hamilton, *J. Mol. Spectrosc.* **184**, 162–166 (1997).
20. S. L. Cheah, Y. P. Lee, and J. F. Ogilvie, *J. Quant. Spectrosc. Radiat. Transfer* **64**, 467–482 (2000).
21. B. Caccin, F. Cavellini, G. Cepatelli, and A. M. Sambuco, *Astron. Astrophys.* **149**, 357–364 (1985).